Fixed-Molecule $1s\sigma_{g,u}$ Photoelectron Angular Distributions as a Probe of σ_g^* and σ_u^* Shape Resonances of CO_2

N. Watanabe,* J. Adachi,† K. Soejima,‡ E. Shigemasa, and A. Yagishita
Photon Factory, National Laboratory for High Energy Physics, 1-1 Oho, Tsukuba-shi, Ibaraki 305, Japan

N. G. Fominykh and A. A. Pavlychev
Institute of Physics, St. Petersburg University, St. Petersburg, 198904, Russian Federation
(Received 14 March 1997)

Angular distributions of $1s\sigma_{g,u}$ photoelectrons from CO_2 molecules, oriented parallel to the electric vector of incident light, have been measured. The angular distribution patters at σ_g^* and σ_u^* shape resonances are significantly different from those expected in the virtual molecular orbitals concept. The analyses of the patterns have made it clear that the mixing of outgoing photoelectron partial waves and the interference between them are responsible for the observed patterns, unlike N_2 photoionization. Calculations based on a quasiatomic model have reproduced the observed patterns fairly well. [S0031-9007(97)03451-0]

PACS numbers: 33.80.Eh

A considerable body of experimental and theoretical works on the soft x-ray photoabsorption for the core level of small molecules has shown that resonances and multielectron effects are commonly encountered [1]. Within the first tens of eV above the core-level ionization threshold, a broad resonance is characteristically found in the photoabsorption spectra, and commonly referred to as a shape resonance because the resonance is due to the temporary trapping of the outgoing photoelectron by a centrifugal molecular potential barrier [2]. In an alternative description, the resonance is due to a transition into an antibonding virtual valence orbital in the continuum [3]. The link between the scattering and molecular orbital concepts is established most elegantly by viewing the multiple scattering wave function [4] as being similar to the contour maps used for picturing molecular orbitals. Thus, the basic phenomenon of the shape resonance is well understood, but only qualitative agreement is found between theory and experiment even for simple diatomic molecules.

In polyatomic molecules, the shape resonance profile can be different, depending on which atomic core level is ionized. Moreover, more than one resonance is generally present, so that not only the spatial localization but also symmetry properties of the shape resonance become important. For example, two shape resonances have been predicted by theory for the K shells of CO_2 [5,6], corresponding to transitions into the virtual antibonding $5\sigma_g^*$ and $4\sigma_u^*$ molecular orbitals. However, dipole selection rules allow only the $4\sigma_u^*$ resonance for C $1s$ ($2\sigma_g$ orbital) photoionization, whereas both resonances can occur for O $1s$ ($1\sigma_g$, $1\sigma_u$) photoionization [7,8]. Indeed, by our symmetry-resolved photoabsorption spectroscopy [9], one can clearly see two shape resonances for the parallel transition component; σ_g^* and σ_u^* resonances at 542 and 559 eV, respectively (see Fig. 1). The purpose of the present work is to probe the continuum wave functions being responsible for the shape resonances of CO_2 experimentally and theoretically. To realize the visualization of the continuum wave functions, we have undertaken the photoelectron angular distribution measurements from fixed-in-space molecules [11–13]. And, to explain our angular distribution patterns, we have also undertaken the theoretical calculations based on a quasiatomic model, i.e., photoionization being regarded as occurring in an atom incorporated into its surroundings [14,15].

The experiments were performed on the beam line BL-2B at the Photon Factory 2.5 GeV storage ring, with the photon energy being selected by a 10-m grazing incidence

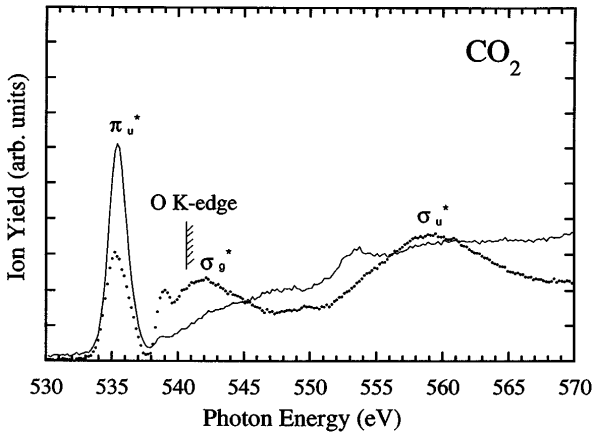

FIG. 1. Symmetry-resolved O K-edge photoabsorption spectra of CO_2. A dotted line spectrum expresses the $\sigma \rightarrow \sigma$ parallel transition component, and a solid line spectrum shows the $\sigma \rightarrow \pi$ perpendicular transition. In the $\sigma \rightarrow \sigma$ spectrum, the σ_g^* and σ_u^* shape resonances are observed at 542 and 559 eV, respectively. It should be mentioned that the symmetry decomposition of excited states is not applicable to the transitions below the ionization threshold of CO_2 [10].

 0031-9007/97/78(26)/4910(4)$10.00

monochromator. The description of the experimental apparatus was reported in detail elsewhere [11,12]. Briefly, the apparatus consists of two identical retarding field analyzers for ion detection, mounted parallel and perpendicular to the polarization vector of the incident light, and a rotatable parallel plate analyzer for electron detection. The method adopted in our study, in order to determine angular distributions from oriented molecules, is attributed to the delayed coincidence technique between angle- and energy-resolved photoelectrons and ions [11–13]. That is, the populations of molecules with the desired orientation were selected by detecting energetic fragment ions ejected either parallel or perpendicular to the polarization vector. The data were acquired at the photon energies of 542 (σ_g^* shape resonance), 547, 550, 554, 559 (σ_u^* shape resonance), and 579 eV. In this paper, we concentrate our discussions on the results of the angular distributions of $1s\sigma$ photoelectrons from CO_2 molecules oriented along the polarization vector.

The angular distributions of $1s\sigma$ photoelectrons are shown in Fig. 2. The experimental data points are shown by filled circles with error bars, and the results of fitting these points by using the least-squares method, whose procedure will be described later, are expressed by the dashed curves. The maximum value is normalized to unity in each pattern. In contrast to the results of N_2 molecules [11,13], the angular distribution patterns at the σ_g^* and σ_u^* resonances significantly differ from the ones expected from the transitions into the antibonding molecular orbitals of $5\sigma_g^*$ and $4\sigma_u^*$ [16], although one can see a little similarity between them, i.e., the maximum and minimum at $\theta = 90°$ for the σ_g^* and σ_u^* resonance, respectively. The reason for the discrepancy is considered to be due to a strong mixing among outgoing partial waves, as discussed by Dittman *et al.* [17] for the valence-shell photoionization of CO_2 molecules. Then these shape resonances would not be induced by a strong enhancement of single channel contribution, such as the N_2 case [11,13]. At the highest photon energy of 579 eV, the angular distribution pattern becomes very similar to the one predicted from the atomic transition of $1s \rightarrow \varepsilon p$. It implies that the molecular potential barrier is almost negligible for the photoelectrons having that high kinetic energy.

In order to investigate these shape resonances quantitatively, we have applied the formulation of fixed-molecule photoelectron angular distributions by Dill [18] and by Cherepkov and Kuznetsov [19] to the analyses of our data. For the photoionization of cylindrically symmetric molecules with the electric vector parallel to the molecular z axis, the fixed-molecule photoelectron angular distributions can be expressed by a series of Legendre polynomials P_K,

$$\frac{d\sigma}{d\hat{\boldsymbol{k}}} = \sum_{K=0}^{2l_{\max}} A_K P_K(\cos\theta), \qquad (1)$$

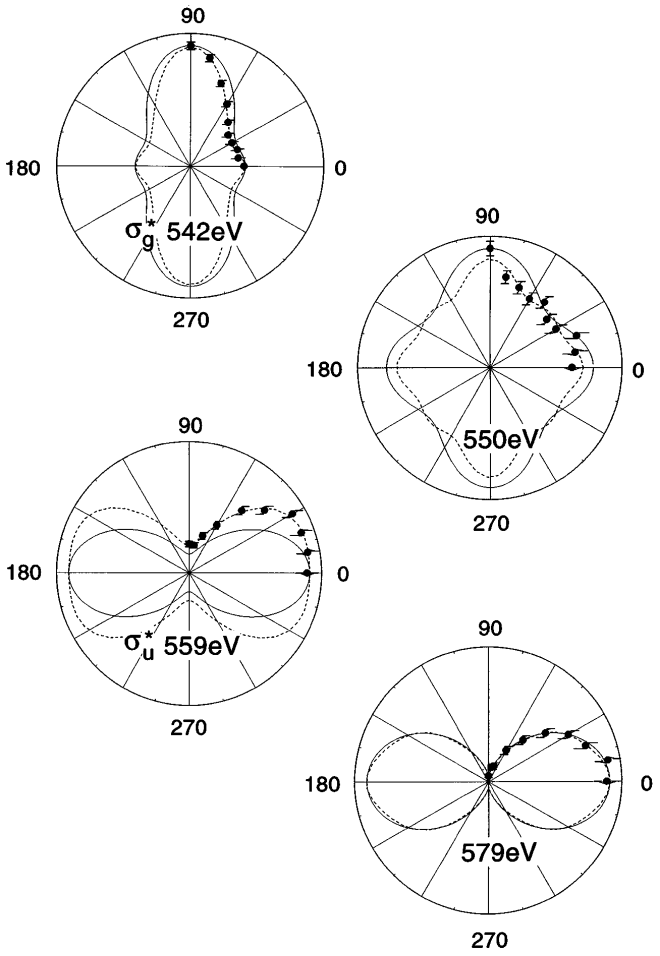

FIG. 2. Polar plots of angular distributions of $1s\sigma_{g,u}$ photoelectrons from CO_2 molecules oriented parallel to the polarization vector, which is directed to the 0°-180° line. Filled circles with error bars represent the experimental data points, and the dashed curves show data points fitted to the experimental data (see text). The dramatic change of the angular distribution patters is observed as a function of photon energies written in the plots. The theoretical results are drawn by the solid curves, which are normalized at the maximum points; strong spd hybridization (542 eV) and weak spd hybridization (559 eV).

where $\hat{\boldsymbol{k}} = \{\theta, 0\}$ is the photoelectron ejection direction measured in the molecular frame. In $D_{\infty h}$ symmetric molecules, such as CO_2, the expansion in Eq. (1) is limited to the even values of K. In the even terms of A_K, the $g \rightarrow u$ and $u \rightarrow g$ transitions do not couple. We take into account the three dominant channels for the $g \rightarrow u$ transitions, $1s\sigma_g \rightarrow p\sigma_u$, $f\sigma_u$, and $h\sigma_u$, and for the $u \rightarrow g$ transitions, $1s\sigma_u \rightarrow s\sigma_g$, $d\sigma_g$, and $g\sigma_g$. Here, one should note that the ungerade symmetry molecular wave functions consist of only odd parity partial waves while the gerade ones consist of only even parity partial waves, because the spatial origin of partial wave functions is set on the center of a molecule. Under this approximation, the expansion coefficients of A_K in Eq. (1) are truncated

by $K = 10$ and given by

$$
\begin{aligned}
A_0 &= \pi\alpha h\nu(|D_s|^2 + |D_p|^2 + |D_d|^2 + |D_f|^2 + |D_g|^2 + |D_h|^2),\\
A_2 &= \pi\alpha h\nu\Big(2|D_p|^2 + \frac{10}{7}|D_d|^2 + \frac{4}{3}|D_f|^2 + \frac{100}{77}|D_g|^2 + \frac{50}{39}|D_h|^2 - 2\sqrt{5}D_s^*D_d\cos\delta_{sd}\\
&\quad - 6\sqrt{\frac{3}{7}}D_f^*D_p\cos\delta_{pf} - \frac{12\sqrt{5}}{7}D_g^*D_d\cos\delta_{dg} - \frac{100}{3\sqrt{77}}D_h^*D_f\cos\delta_{fh}\Big),\\
A_4 &= \pi\alpha h\nu\Big(\frac{18}{7}|D_d|^2 + \frac{18}{11}|D_f|^2 + \frac{1458}{1001}|D_g|^2 + \frac{18}{13}|D_h|^2 + 6D_g^*D_s\cos\delta_{sg} - 8\sqrt{\frac{3}{7}}D_f^*D_p\cos\delta_{pf}\\
&\quad - \frac{120\sqrt{5}}{77}D_g^*D_d\cos\delta_{dg} + 10\sqrt{\frac{3}{11}}D_h^*D_p\cos\delta_{ph} - \frac{360}{13\sqrt{77}}D_h^*D_f\cos\delta_{fh}\Big), \qquad (2)\\
A_6 &= \pi\alpha h\nu\Big(\frac{100}{33}|D_f|^2 + \frac{20}{11}|D_g|^2 + \frac{80}{51}|D_h|^2 + \frac{12\sqrt{33}}{11}D_h^*D_p\cos\delta_{ph}\\
&\quad - \frac{30\sqrt{5}}{11}D_g^*D_d\cos\delta_{dg} - \frac{14\sqrt{77}}{33}D_h^*D_f\cos\delta_{fh}\Big),\\
A_8 &= \pi\alpha h\nu\Big(\frac{490}{143}|D_g|^2 + \frac{490}{247}|D_h|^2 - \frac{112\sqrt{77}}{143}D_h^*D_f\cos\delta_{fh}\Big),\\
A_{10} &= \pi\alpha h\nu\Big(\frac{15\,876}{4199}|D_h|^2\Big),
\end{aligned}
$$

where α is the fine structure constant, D_l is the dipole matrix element for the transition into the εl continuum state, and $\delta_{ll'}$ is the phase difference between εl and $\varepsilon l'$ partial waves. We have determined the relative values of A_K by the fitting procedure using Eq. (1) with $K \leqq 10$. The dashed curves in Fig. 2 show the least-squares fits. The values of A_K are listed in Table I. The uncertainties of the values have been evaluated to be less than 30%. If the σ_g^* shape resonance is predominated by the $g(l = 4)\sigma_g$ partial wave as predicted from the angular variation of the $5\sigma_g^*$ molecular orbital around the molecular center at the large distance from it [16], one can expect an enhancement of the A_8 coefficient at 542 eV, such as in N_2 photoionization [11,13]. And, similarly, if the σ_u^* shape resonance is dominated by the $h(l = 5)\sigma_u^*$ partial wave as expected from the $4\sigma_u^*$ orbital [16], one can assume an increase of A_{10} at 559 eV. However, as can be seen in Table I, this is not the case. From further inspection of Table I, one recognizes that the coefficients A_2 and A_6 are negative at 542 eV. It implies that the interference terms among outgoing partial waves [see Eq. (2)] contribute appreciably to the angular distribution pattern at the σ_g^* shape resonance. In the same way, the negative values of A_4 and A_6 at 559 eV indicate that the interference effect is important at the σ_u^* shape resonance. By numerical analyses, we can conclude that both the mixing of the outgoing partial waves and the interference effects among them are responsible for the observed patterns. Therefore, one cannot find a one-to-one correspondence between single orbital momenta and eigenchannels in contrast to N_2 photoionization.

To give a practical interpretation for the observed angular distribution patterns, we described them by using the quasiatomic model [14,15]: The O K-shell photoionization of CO_2 molecules is considered a photoionization of a single oxygen atom, which is modified by the surroundings' potential. The strong localization of the K-shell hole reduces the ground state molecular symmetry of $D_{\infty h}$ to that of $C_{\infty h}$, and induces the local dipole moment. One can construct the σ_g^* and σ_u^* eigenchannels by the even and odd linear combinations of the K-shell excitations of left and right terminal oxygen atoms.

TABLE I. Expansion coefficients A_K of Legendre polynomials in Eq. (1). A_0 is normalized to unity. E_k denotes the kinetic energy of photoelectrons in eV.

Photon energy (eV)			A_0	A_2	A_4	A_6	A_8	A_{10}
542.0	σ_g^*	($E_k = 1.2$)	1.0	−0.67	0.42	−0.11	0.07	0.007
547.0		($E_k = 6.2$)	1.0	−0.45	0.67	−0.41	0.12	∼0
550.0		($E_k = 9.2$)	1.0	−0.15	0.25	−0.11	0.19	∼0
554.0		($E_k = 13.2$)	1.0	0.43	0.16	−0.02	0.07	∼0
559.0	σ_u^*	($E_k = 18.2$)	1.0	1.14	−0.18	−0.16	0.03	0.01
579.0		($E_k = 38.2$)	1.0	1.69	−0.004	−0.06	0.01	0.09

Our calculations of the photoelectron angular distributions have shown that the intramolecular interference magnifies resonantly the pl-hybridization effect on the parallel transitions from the O K-shell, which controls the direction of photoelectron current. From Eq. (1) in Ref. [15], the contribution of an l harmonic to the photoelectron wave function is expressed by $A_{pl\sigma} = [T/(1 - BS)]_{pl\sigma}$, where S is a scattering matrix, and B and T are the matrices describing reflection and transmission through the surroundings, respectively. The calculated angular distribution patterns, with the hybridization among s-, p-, and d-partial waves taken into account, are plotted in Fig. 2 for four photon energies, including the σ_g^* and σ_u^* resonances. The degrees n_l of the spd hybridization are given in Table II. The n_l are normalized to give the unity in the sum. The hybridization is the highest at the lowest photon energy corresponding to the σ_g^* resonance, and it decreases with an increase of photon energy. The calculated angular distributions reproduce the experimental trend shown in Fig. 2 fairly well. The agreement between theory and experiment implies that the spd hybridization at the σ_g^* and σ_u^* resonances plays a central role in the photoelectron angular distributions. As the multiple scattering decreases with the increase of photoelectron kinetic energy, the hybridization in the σ_u^* resonance is weaker than that in the σ_g^*. To assist the understanding of the increase of the hybridization with the decrease of photoelectron velocity, it is helpful to introduce the pseudopotential concept. For low-energy photoelectrons, the intramolecular interference leads to the blocking of their transmission through the surrounding C-O fragment. Thus, the destructive interference effect of photoelectrons can be modeled by a potential barrier at the location of the fragment. Then, it is supposed that the surroundings' anisotropy is energy dependent and enhanced for low-energy photoelectrons, giving rise to a strong spd hybridization. In accordance with this qualitative explanation, at the highest photon energy 579 eV, where the interference becomes fairly weak, the angular distribution in the σ channel approaches the one described by the p_z function. On this background, the observed patterns can be rationalized from the viewpoint that the local electron optical properties (the relief of the surroundings' pseudopotential) define the major direction of photoelectron emission.

We would like to acknowledge Professor N. Kosugi and Professor N. A. Cherepkov for their fruitful discussion and comments on theoretical treatment. We are grateful to the staff at the Photon Factory for the stable operation of the storage ring. This work has been performed under approval of the Photon Factory Advisory Committee (Proposals No. 93G311 and No. 95G369). The quasiatomic research was supported by RFFI (95-03-033138a).

TABLE II. The degree of the spd hybridization in the computed angular distribution patterns shown in Fig. 2.

Photon energy (eV)		n_s	n_p	n_d
542.0	σ_g^*	0.51	0.28	0.21
550.0		0.48	0.28	0.24
559.0	σ_u^*	0.31	0.50	0.19
579.0		0.08	0.72	0.20

*Permanent address: The Institute of Low Temperature Science, Hokkaido University, Sapporo, Hokkaido 060, Japan.
†Permanent address: Institute for Molecular Science, Myodaiji, Okazaki 444, Japan.
‡Permanent address: Graduate School of Science and Technology, Niigata University, 8050 Ikarashi, Niigata-shi, Niigata 950-21, Japan.

[1] A. P. Hichcock, J. Electron Spectrosc. Relat. Phenom. **25**, 245 (1982).
[2] J. L. Dehmer, D. Dill, and A. C. Parr, *Photophysics and Photochemistry in the Vacuum Ultraviolet*, edited by S. McGlynn, G. Findly, and R. Huebner (D. Reidel Publishing Company, Dordrecht, 1985), p. 341.
[3] F. A. Gianturco, M. Guidotti, and U. Lamanna, J. Chem. Phys. **57**, 840 (1972).
[4] D. Loomba, S. Wallence, D. Dill, and J. L. Dehmer, J. Chem. Phys. **75**, 4546 (1981).
[5] N. Padial, G. Csanak, B. V. McKoy, and P. W. Langhoff, Phys. Rev. A **23**, 218 (1981).
[6] W. R. Daasch, E. R. Davidson, and A. U. Hazi, J. Chem. Phys. **76**, 6031 (1982).
[7] R. G. Wight and C. E. Brion, J. Electron Spectrosc. Relat. Phenom. **3**, 191 (1974).
[8] V. N. Sivkov, V. N. Akimov, and A. S. Vinogradov, Opt. Spectrosc. **63**, 275 (1987).
[9] A. Yagishita, E. Shigemasa, J. Adachi, and N. Kosugi, in *Proceedings of the 10th International Conference on Vacuum Ultraviolet Radiation Physics*, edited by F. J. Wuilleumier, Y. Petroff, and I. Nenner (World Scientific, Singapore, 1993), p. 201.
[10] J. Adachi, N. Kosugi, E. Shigemasa, and A. Yagishita, J. Phys. Chem. **100**, 19 783 (1996).
[11] E. Shigemasa, J. Adachi, M. Oura, and A. Yagishita, Phys. Rev. Lett. **74**, 359 (1995).
[12] P. A. Hatherly, J. Adachi, E. Shigemasa, and A. Yagishita, J. Phys. B **28**, 2643 (1995).
[13] E. Shigemasa, J. Adachi, M. Oura, N. Watanabe, K. Soejima, and A. Yagishita, *Atomic and Molecular Photoionization*, edited by A. Yagishita and T. Sasaki (Universal Academy Press, Inc., Tokyo, 1996), p. 69.
[14] A. A. Pavlychev, A. S. Vinogradov, A. P. Stepanov, and A. S. Shulakov, Opt. Spectrosc. **75**, 554 (1993).
[15] A. A. Pavlychev and N. G. Fominykh, J. Phys. Condens. Matter **8**, 2305 (1996).
[16] W. L. Jorgensen and L. Salem, *The Organic Chemist's Book of Orbitals* (Academic Press, New York, 1973), p. 131.
[17] P. M. Dittman, D. Dill, and J. L. Dehmer, Chem. Phys. **78**, 405 (1983).
[18] D. Dill, J. Chem. Phys. **65**, 1130 (1976).
[19] N. A. Cherepkov and V. V. Kuznetsov, Z. Phys. D **7**, 271 (1987).